CHARACTERIZING A SOLENOID LENS FOR AN ELECTRON BEAM LINAC

An Undergraduate Research Scholars Thesis

by

CHRISTIAN RATCLIFF

Submitted to the LAUNCH: Undergraduate Research office at
Texas A&M University
in partial fulfillment of the requirements for the designation as an

UNDERGRADUATE RESEARCH SCHOLAR

Approved by
Faculty Research Advisor: Dr. Peter McIntyre

May 2023

Major: Physics

RESEARCH COMPLIANCE CERTIFICATION

Research activities involving the use of human subjects, vertebrate animals, and/or biohazards must be reviewed and approved by the appropriate Texas A&M University regulatory research committee (i.e., IRB, IACUC, IBC) before the activity can commence. This requirement applies to activities conducted at Texas A&M and to activities conducted at non-Texas A&M facilities or institutions. In both cases, students are responsible for working with the relevant Texas A&M research compliance program to ensure and document that all Texas A&M compliance obligations are met before the study begins.

I, Christian Ratcliff, certify that all research compliance requirements related to this Undergraduate Research Scholars thesis have been addressed with my Faculty Research Advisor prior to the collection of any data used in this final thesis submission.

This project did not require approval from the Texas A&M University Research Compliance & Biosafety office.

TABLE OF CONTENTS

Page

ABSTRACT

Characterizing a Solenoid Lens for an Electron Beam LINAC

Christian Ratcliff
Department of Physics & Astronomy
Texas A&M University

Faculty Research Advisor: Dr. Peter McIntyre
Department of Physics & Astronomy
Texas A&M University

Electron beam technology is a growing field with applications in industrial processes, the medical field, and the physical sciences. To accelerate the electrons to the required energy, they are sent through a linear accelerator, which electric fields to accelerate the charges, and uses magnetic fields to channel them through the accelerator aperture. In order to effectively channel the electron beam in its transport, solenoid magnets are used. A solenoid is an asymmetric winding of insulated turns of copper foil strip, wound onto an insulating mandrel. When the current is driven through the winding, it produces an asymmetric distribution of field that threads through the aperture and returns it outside. The electrons are deflected in the gradient fields before and after the solenoid, and are alternately focused and defocused as they move along the axis.

First a custom apparatus was constructed to measure the field flux and current pulse properties, were then analyzed to extract the central field strength for a given current and the spatial distribution of magnetic fields along the axis. Next a prior derivation of the magnetic field flux was adapted to fit the specifications of the solenoid, and compared to the data that was collected. A numerical simulation code, COMSOL, was used to simulate the magnetic field flux, and the results were compared to the measurements. Utilizing the principle of superposition, a beam line containing 14 identical solenoid lenses was simulated using the data gathered from one solenoid.

The focal length of the solenoid was measured to be 1.31 m. Finally the path of an electron was simulated though the beam tube in order to establish the focal properties of the beam transport. Ensuring the exact output location of the electron from the input location is of paramount importance as it reduces the overall uncertainty in the final data.

ACKNOWLEDGMENTS

Contributors

I would like to thank my faculty advisor, Dr. Peter McIntyre, and my thesis advisor for this project, and my research advisor for the past 3 years, for their guidance and support throughout the course of this research.

I would also like to thank Gareth May, the graduate student in charge of this project, for helping me with every step of this project, and guiding me to the best way to accomplish things, while also giving me space to work through problems on my own. I would also like to thank Tim Elliot, our lab's Senior Scientific Instrument Maker, for helping me assemble all of the equipment I used while undertaking this project, as well as helping me better understand the design process of the solenoid. Thanks also go to Cannon Coats and John Rogers for always being willing to be sounding boards for my ideas, as well as helping with any questions I may have had. Finally thanks go to Connor Bowerman, my fellow undergraduate on this project, in helping me with data collection and data processing.

The materials used for, Characterizing a solenoid of an electron beam tube, were provided by Accelerator Research Laboratory (ARL) at Texas A&M.

All other work conducted for the thesis was completed by the student independently.

Funding Sources

Undergraduate research was supported by Accelerator Research Laboratory at Texas A&M University and an additional help from Accelerator Technology Corp in College Station, Texas.

This work was made possible in part with funding from Lawerence Livermore National Laboratory.

1. INTRODUCTION

When designing an electromagnet for a practical application, it is necessary to formulate the magnetic field distribution that would provide the desired effect for the application, and then to design an arrangement of current-carrying windings (and for some applications a steel flux return) that can produce such a distribution. For the present application an array of pulsed solenoids will be used to transport an energetic electron beam. The magnet field is produced by passing electric current through a winding, which will transport the electrons throughout the array.

1.1 Magnetic field representation

The distribution of the magnet field produced due to a solenoid is traditionally approximated by the use of an infinite solenoid, but that is not helpful for this use. An infinite solenoid is a useful first approximation as its infinite length allows for all edge effects to be ignored; that is all the complicated and non-uniform at the end of the solenoid. It also means that the magnetic fields are uniform across the circular cross-section of the solenoid. This is a helpful approximation because it means that wherever the charge enters in solenoid, it will behave in exactly the same way. Obviously this is an easier way to solve a problem, but it is much less realistic. The solenoid that will be used is not a traditional solenoid, where a thin wire is wrapped in a coil, analagous to a spring. Instead it is a wide and flat tape, whose width is the length of the solenoid, that is wrapped in successive layers, in a fashion much like how a roll of tape looks. To theoretically calculate the magnetic field of a similar solenoid, a group of engineers at NASA has developed a system of equations for accurately describing the field utilizing Maxwell's equations [1]. However this is not exactly what is needed, as it only describes a single turn of solenoid, so their equation will be modified to account of the loops of increasing radius.

COMSOL is software that is capable of numerically solving many coupled partial differential equations and simultaneous simulations of different physical systems. In this software a 3D replica of the solenoid will be created, including the material composition of the solenoid and

the physical dimensions of the winding. It is important to include the proper material as different materials can have widely different magnetic characteristics, which will be demonstrated later in Sec. 2.2.1.1. The reason the physical dimensions are imporant and not just the relative shape is because not all physical processes scale linearly, and an observed effect at one size, will be double in strength at double the size, instead it could be x4 the strength, or x$\sqrt{2}$ the strength. Having the correct dimensions allows us not only to do one-to-one comparisons with the measured data, it also allows for the correct physics to be simulated. A group of researchers working on the Mu2e experiment has shown that COMSOL is an effective means of modeling these magnetic fields of a solenoid [2]. They generated these predictions in COMSOL, and then performed a similar process of measuring the magnetic field with a Hall probe, and compared the two results. They found that with the correct boundary conditions in a meshed 2D or 3D space, they were able to accurately model the correct fields. COMSOL will be used in a similar fashion in this project, and results will be plotted together to determine the difference between the theoretical calculations and the COMSOL predictions.

Another method to do this is to collect data in relatively few spots, and the magnetic fields can be recreated by utilizing the solutions to Maxwell's equations in an helical coordinate system [3]. This was done by a group at Northwestern, and they were able to recreate the magnetic fields accurately. This will serve as an additional check of the fields found by NASA and COMSOL, as they should all be generating the same result.

1.2 Solenoid Focusing

Solenoid focusing is when a solenoidal magnet is used to bend energy beams in a way that is very similar to the way glasses refract the light going into the eye. Characterizing the properties of this "lens" is what this study aims to do. Solenoid focusing is an explored area, with equations already have been developed to model the flight of a charge through the magnetic field of a solenoid [4]. These equations were solved generally, and must be altered to fit the parameters of the apparatus, and a program must be developed to model the path of an electron. These focal properties of the solenoids will then be used by researchers at Lawerence Livermore National Lab

(LLNL) to focus a beam of electrons into a single beam of a fixed radius and all in the same direction. Careful measurement and calculation of these properties is paramount, as these the precision of these parameters will effect the overall error of the completed experiment at LLNL.

2. METHODS

There are multiple phases to this experiment: designing of the measuring apparatus, mapping the magnetic field of the solenoid, development of the theoretical model, generation of COMSOL solutions, comparison of the three methods, and finally simulating the path of the electron through the tubes and measurement of the lens factor.

2.1 Background Knowledge

Instrumental to the comprehension the contents of this investigation are knowledge and understanding of magnetic fields, and how an electron interacts with it. A magnetic field is a region that surrounds some sort of magnetic source that describes how charges, currents, or other magnetic materials are influenced via the electromagnetic force. As the electron enters a magnetic field, the electron experiences a force (Lorentz force), that is perpendicular to both the initial direction the electron and the direction of the magnetic field. It is necessary to know that the magnetic field does not accelerate the electron, it merely changes the direction. The electric field is what accelerates an electron. The electric field lines start at an area of high charge, and point towards the area of low charge. The electron moves perpendicularly to these electric field lines, but they are accelerated in the direction opposite that the lines are pointing, because their charge is negative.

2.2 Development of the measuring apparatus

The measurement apparatus contains two main parts: the physical structure and the software that captures the data. These two parts of the system were developed independently, and then were finally assembled together, once both were independently tested.

2.2.1 Physical structure of measuring apparatus

The laboratory already possessed a Coordinate Measuring Machine (CMM), which allows precise placement in each of the three cartesian dimensions. The probe that was used to measure the field was the Senis Magnetic Field Transducer, Three-Axis, F3A type C [5]. This probe is capable of measuring magnetic fields from 0 T to $\pm$ 2 T. The area of the probe which is capable

of sensing magnetic field is 0.00025 mm^3 in area, small enough so that it can be considered as a single point, and this point is at a location specified in the manual. A custom mount was machined that holds the probe in a specific location, while also protects it in case of accidental bumps with the solenoid. The probe mount in connected to the CMM by a tube of brass; the brass allows a sturdy connection while also not affecting any of the magnetics. The probe was placed such that the observation point was placed at r=0 on one of the open faces of the solenoid. This starting location was defined as (0,0).

2.2.1.1 Designing the Mandrel

Initially a bronze mandrel was used to wind the magnet around. A problem arose when this inner bronze ring was essentially functioning as a single loop coil, which was inside of the copper tapes that made up the solenoid. The initial flux density measurements revealed that the value was much lower than expected, and an investigation was undertaken to determine the cause.

The first thing that was tested was accuracy of the Hall Probe. By taking a simple copper wire and wrapping it around a PVC pipe of approximately the same diameter of the solenoid the rough approximation of the solenoid's fields could be recreated. It was found that fields matched what they were expected to be, so the Hall Probe could confidently said to be in working order.

This left only the solenoid itself and its structure as the only remaining cause of the issue. It was then when a member of the group raised the point that since this is a pulsed solenoid, not a DC solenoid, the bronze ring inside is acting like a second coil. A pulsed solenoid means that the current delivered to the solenoid was in the form of a pulse; it increased from a zero-point, reached a max, and then descended, much like how a hill on a roller coaster functions. A DC solenoid means that the current delivered is direct current (DC), meaning it was at a constant value in a constant direction, in contrast to alternating coil (AC) where the current direction rapidly changes directions back and forth, hundreds to thousands of times a second. As it uses a pulsed current, this generates a number of complications which were not immediately seen.

Arising from Maxwell's Equations, Eq. 1 is Faraday's Law of Induction, Eq. 4, in which is contained Lenz's Law. Lenz's Law states, "Nature abhors a change in flux. The induced current

will flow in such a direction that the flux it produces tends to cancel the change" [6]. Flux is the rate of flow of anything through a specified surface or area. The amount of magnetic field lines passing through a cross-sectional area is the magnetic flux of that object.

$$\vec{\nabla} \times \vec{E} = -\frac{\partial \vec{B}}{\partial t} \tag{1}$$

$$\oint_{\partial S} \vec{E} \cdot \mathrm{d}\vec{l} = -\int_S \frac{\partial \vec{B}}{\partial t} \cdot \mathrm{d}\vec{A} \tag{2}$$

$$= -\frac{\mathrm{d}}{\mathrm{d}t} \int_S \vec{B} \cdot \mathrm{d}\vec{A} \tag{3}$$

$$\mathcal{E} = -\frac{\mathrm{d}\Phi_B}{\mathrm{d}t} \tag{4}$$

In other words, the induced current will create a new magnetic field that points in the opposite direction of the original magnetic field. The current was passing over the solenoid's copper rings and generating a magnetic field as it was supposed to do, but this field was inducing a current in the inner bronze ring, which in turn created a magnetic field, pointing in the opposite direction of the copper coil's field. It is a principle of superposition that any field can be decomposed into many different fields that all sum to the original, and that is what is happening here. The main field is pointing in one direction, and the induced field is in the opposite direction, and when they sum together, their total field is roughly half of the intended.

These induced fields are a problem with pulse magnets as it is a nature of a pulse to have one big change, so the induced fields can be quite large. Traditionally this is mitigated by introducing an air gap in the inner coil, preventing it from creating a circuit and allowing current to flow. This is one of the options that the group explored; the other being changing the inner coil to be made of a non-magnetic material. After protoyping an air gap mandrel, ultimately the group decided for ease of fabrication that the mandrel material would be switched to G10, a fiberglass resin laminate. Fiberglass has no magnetic properties, therefore eliminating the prior issues.

2.2.2 Software for the recording of the field data

The SENIS Hall Probe outputs eight channels of data; $\pm B_x$,$\pm B_y$, $\pm B_z$, and two channels for temperature data. These later two channels were disregarded as they are not necessary to the experiment [5]. The probe streams data up to 25 kHz, and that sampling rate that was chosen, meaning data was taken 25000 times per second. Initially the plan was to use a data acquisition device (DAQ), and specifically the LabView T7 was in consideration, but an issue was discovered with the allocation of sampling rate that necessitated alternate solutions. If this device were to be used, the theoretical maximum of the sampling rate would be used, but in a realistic scenario, 100% of the sampling rate was not available, and significant data loss would have occurred. A lesser sample rate was not feasible since the entire width of the pulse is milliseconds in length, and the length of the plateau is on the scale of hundreds microseconds. If we wanted to get enough samples of the plateau, the 25 kHz sampling rate was needed.

In order to mitigate this issue, the method of data collection changed. A RIGOL DS1054Z Oscilloscope was used as the instrument for data collection, with differential amplifiers on all of the input channels. These differential amplifiers took the difference between the two signals and recorded that value as the measured field. The data stream mode was open, and a collection of values at 1200 time steps were taken, at 10 μs intervals. These data points were then manually saved to a CSV file on a USB drive, and then transferred to a storage drive. A new file was made for each observation point.

2.3 Mapping of the magnetic field of the solenoid

2.3.1 Physically Mapping the Field

As one of the primary points of this project is to verify that the fields match those generated in simulation, every single point in the solenoid will not be mapped; instead a selection of points are chosen. Setting z=0 at one face of the solenoid, points were taken from $z = -85$ mm to $z = 85$ mm, at three radii, r =0, 10, and 20 mm. Most of the points taken at r =10 and 20 mm were taken on one side of the solenoid, but additional points were at the same radius, 180° offset to verify that there were no asymmetries in the field. These additional points were taken in 25mm increments

not 5 mm. All data points were collected within the same two hour bloc, in an effort to keep any external factors consistent.

There are two configurations of the solenoid that were measured: with the physical beam tube inside the solenoid, and without the beam tube. As the beam tube is made of metal, it is expected that it will have some effect on the fields, so it is important to characterize this difference. The same data points were taken with both configurations, and these were also taken within the same two hour bloc.

2.3.2 Translating Data into Readable Charts

The first step in the data processing portion of this project was taking the thousands of data points for the magnetic field in each of the three dimensions, isolating the plateau at the peak of the pulse, averaging over the entire plateau, and outputting that single, averaged field value for each of the three dimensions, at each location point. The size of the pulse plateau was already known, 200 μs, so the finding the peak is the priority. First each file is input into Python, and each column of data is isolated and appropriately sorted. By looking at the plot of the magnetic flux density vs time data, there was consistently a range where the peaks fell, such as in Fig 1.

To make the computational time faster, a narrow range was chosen instead of the entire 1200 data points, seen in Fig 1. Then both the B_z and the current narrowed data were put through a Savitzky-Golay (Savgol) Filter to help reduce the noise, as it was initially extremely turbulent. A Savgol Filter takes subsets of data points that are adjacent to one another, and uses a least squares fit (a type of approximation) to approximate data point locations. When each data point is equidistant from its two adjacent points, the least square fit equations can be solved to get a set of convulation coefficients. These coefficients can then be applied to each subset of data points, passing the entire set of data through this filter, smoothing out the data [7]. This comparison can be seen in Figs. 2 and 3. The narrowed and smoothed data now closely resembled a parabolic curve. A program was written to trace the parabolic curve and identify the peak, average a range of 21 data points centered at the peak, and that value was what was given as the magnetic flux value.

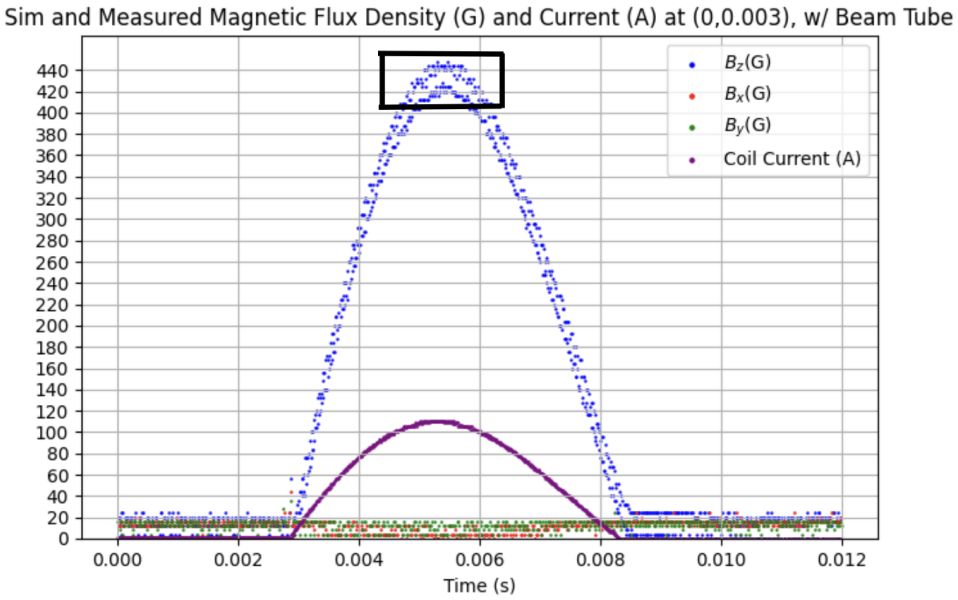

Figure 1: *Graphical representation of the data collected at a single current pulse, when the probe was located at 0.005 m into the solenoid. The black box is meant to emphasize the region that will be utilized to find the peak of the current.*

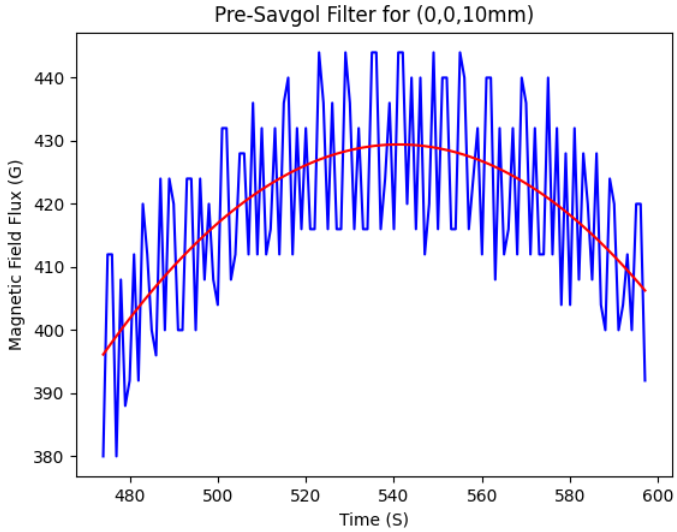

Figure 2: *This is the top of the magnetic field peak. The actual data is in blue, and the red line is the estimated best fit line. This is before the Savgol filter is applied.*

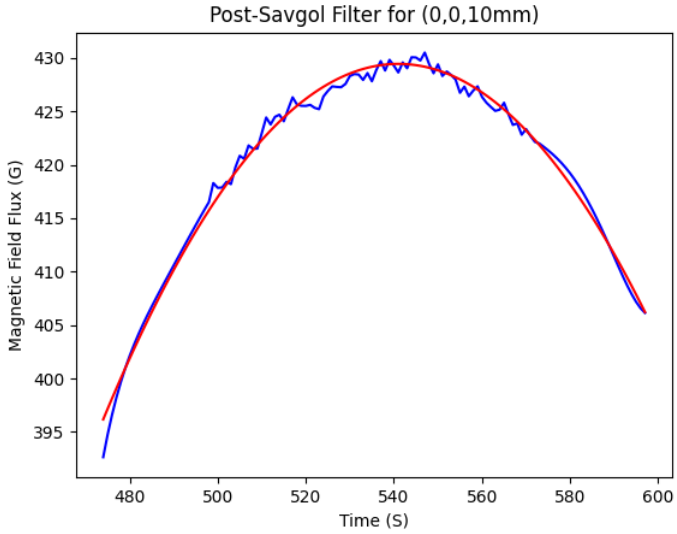

Figure 3: *This is the exact same data from Fig. 2 except the measured data has been processed through a Savgol filter and a new best fit line has been drawn.*

2.4 Development of the theoretical model

Development of a theoretical model begins with an ideal case, and from there becomes more and more general. The general case is that of an infinite solenoid, which is a solenoid that is so long, the edge effects do not exist, and the field is uniform across the cross section of the bore axis, and the field only points in the direction of the bore axis. From here on, the coordinate system will be redefined for simplicity. No longer is $z = 0$ at the face of the solenoid, instead $z = 0$ lies in the middle of the solenoid. Its magnetic field equation can be seen in Eq. 5

$$B_z\left(r = 0, z\right) = B_0\left(z\right) = \frac{\mu_0 I}{2L}\left[\frac{z + L/2}{\sqrt{(z + L/2)^2 + R^2}} - \frac{z - L/2}{\sqrt{(z - L/2)^2 + R^2}}\right] \tag{5}$$

This field was adapted first by taking the equations by NASA, and modifying them to account for the changing radius. Each turn of the solenoid meant that the outer radius of the solenoid increased by the thickness of the copper. For one turn this might not seem like much of a difference, but stack up 54 turns, that is a significant difference in radius. There are two methods of treating this. The first is simply picking the middle point, and treating it as a single radius. The

other way is to design the field equation to be dependent on the number of turns, and after iterating over each turn, summing all the values together. The former method is easier, but the later is more accurate, so that is what will be used. This is just a starting point, used to compare the measured values to the simulated and the predicted values. When it comes time to model the path of the electron through the solenoid, a more rigorous treatment of the fields must occur.

2.5 Generating COMSOL solutions

Within COMSOL a 3D mock-up of the solenoid was made, and many of the experiment parameters are input into the system. This parameters include the material composition, the physical dimensions, and the value of the current. The current value that was input came from the value that was measured at the peak field at each point. Another important factor when designing these simulations is the mesh size. The mesh is how the computer breaks up the system into little parts, and its those parts that the software uses to simulate the physics. The finer the mesh, the more accurate results, but there is a point where diminishing returns are reached. If the value only gets 0.0001% more accurate, but it takes 10 hours to run, that is much less useful that an number accurate to 0.1%, but only takes 30 minutes to run. One of the points of this project is to verify that the simulations are correct, so a very high degree of accuracy is not needed. Therefore a less fine mesh was chosen, and the simulations ran, on average, for 20 minutes. Then the output parameters are set, so that it knows what exactly it is trying to solve for, and then it numerically solves for them. These results are then output into a CSV file, which is then input into the same graphing program as the measured data.

2.6 Comparison of measured field, COMSOL fields, and theoretical fields

The three sets of field data: measured, simulated, and predicted, all used the same current, the current collected during the gathering of the measured data. This allows for a strict comparison of the $\vec{B}$ fields and nothing else. The simulated values that were exported from COMSOL and the values predicted and output from the program are plotted on the same graph as the measured values, so that an easy comparison can be made. It is expected that all three fields will be very close in values to each other.

2.7 Simulating path of electron and measuring lens factor

This derivation in this section was performed in [4].

An important term in solenoid focusing, and accelerator physics as a whole, is rigidity $[B\rho]$. Rigidity is a measure of the stiffness of a beam, or measuring how much angular deflection results when a particle travels through a given magnetic field [8]. In equation form it is [4]:

$$[B\rho] = \frac{p}{q} = \frac{mv\gamma}{q} = \frac{mc}{q}\beta\gamma = \frac{mc}{q}\sqrt{\left(\frac{\mathcal{E}}{mc^2}\right)^2 + 2\left(\frac{\mathcal{E}}{mc^2}\right)} \tag{6}$$

First, the world of the infinite solenoid approximation must be left behind, and more realistic field must be found. The solenoid approximation will not be completely left behind, it instead be the field only along the bore axis, where $r = 0$. Now the radial field must be found, and that derivation is:

$$\vec{B} = B_r\left(r, z\right)\hat{r} + B_z\left(r, z\right)\hat{z} \tag{7}$$

$$\vec{\nabla}\cdot\vec{B} = 0 \Rightarrow \frac{1}{r}\frac{\partial}{\partial r}\left(rB_r\right) + \frac{\partial B_z}{\partial z} = 0 \tag{8}$$

$$\vec{\nabla}\times\vec{B} = 0 \Rightarrow \left(\frac{\partial B_r}{\partial z} - \frac{\partial B_z}{\partial r}\right)\hat{\theta} = 0 \tag{9}$$

$$B_z = B_z\left(r = 0, z\right) + \cdots \approx B_z\left(r = 0, z\right) \tag{10}$$

$$B_r = -\frac{1}{2}B_z'\left(r = 0, z\right) + \cdots \approx -\frac{1}{2}B_z'\left(r = 0, z\right) \tag{11}$$

By assuming that the particles enter from a region where $\vec{B} = 0$, the system is rotationally symmetric, so the canonical momentum ($\mathcal{P}$) is conserved, meaning that it is constant. Canonical momentum is made up of two different momentums; the kinetic and the potential momentums. The kinetic momentum is the momentum that is clearly visible in everyday life; a baseball that is thrown at given velocity, the momentum is equal to the mass of the baseball times the velocity it was thrown at. The potential momentum is harder to describe as it really does not have an everyday analogue. It is similar to the scalar electric potential, where the scalar field is related to the electric field. The magnetic vector potential is similar, except it is a vector field that is related to the

magnetic field. So the potential momentum is the momentum imparted upon the electron by this vector potential. Canonical momentum is the total momentum, summing the kinetic momentum, and the potential momentum. If the beam is initially magnetized then $\mathcal{P} = 0$. Using $A_\theta = \frac{1}{2}B_z(r = 0, z)$ and the fact that $\vec{B} = \vec{\nabla} \times \vec{A}$ it can be shown that:

$$\mathcal{P}_\theta = m\gamma r v_\theta + \frac{qr^2 B_z(r = 0, z)}{2} = \text{constant} \tag{12}$$

$$\mathcal{P}_\theta = 0 \Rightarrow v_\theta = -\frac{qrB_z(r = 0, z)}{2} \tag{13}$$

Now the radial equation of motion can be developed, starting from the Lorentz force law [6].

$$\frac{\mathrm{d}\vec{p}}{\mathrm{d}t} = q\vec{v} \times \vec{B} \tag{14}$$

$$m\gamma\ddot{\vec{x}} = q\dot{\vec{x}} \times \vec{B} \tag{15}$$

$$\Rightarrow m\gamma\left(\ddot{r} - r\dot{\theta}^2\right) = q\left(\dot{r}\hat{r} + r\dot{\theta}\hat{\theta} + \dot{z}\hat{z}\right) \times \left(-\frac{1}{2}B_r\hat{r} + B_z\hat{z}\right) \cdot \hat{r} \tag{16}$$

$$\ddot{r} - r\dot{\theta}^2 = \frac{q}{\gamma m}\left(r\dot{\theta}\right) B_z(r = 0, z) \tag{17}$$

$$\ddot{r} - \left(\frac{qB_z\left(r = 0, z\right)}{2m\gamma}\right)^2 r = -2\left(\frac{qB_z\left(r = 0, z\right)}{2m\gamma}\right)^2 r \tag{18}$$

$$\ddot{r} + \left(\frac{qB_z\left(r = 0, z\right)}{2m\gamma}\right)^2 r = 0 \tag{19}$$

Then the equation is then parameterized in terms of z, rather than t, and using the prior definition for rigidity:

$$\frac{\mathrm{d}}{\mathrm{d}t} = \frac{\mathrm{d}z}{\mathrm{d}t}\frac{\mathrm{d}}{\mathrm{d}z} = v_z\frac{\mathrm{d}}{\mathrm{d}z} \approx v\frac{\mathrm{d}}{\mathrm{d}z}$$

$$[B\rho] = \frac{mv\gamma}{q}$$

Implementing these changes into Eq. 19 becomes:

$$v^2 \frac{\mathrm{d}^2}{\mathrm{d}z^2} r + \left(q \frac{B_z\left(r=0,z\right)}{2m\gamma} \right)^2 r = 0 \tag{20}$$

$$\frac{\mathrm{d}^2}{\mathrm{d}z^2} r + \left(\frac{B_z\left(r=0,z\right)}{2[B\rho]} \right)^2 r = 0 \tag{21}$$

Eq. 21 is in the form of Hill's Equation, which is a second order differential equation that has a periodic coefficient. This periodic coefficient is why the magnetic field causes the electron to spiral around the z-axis [4].

Eq. 21 can also be reached in another way, by considering the geometry of the solenoid. Even though it reaches the same conclusions, seeing the system as a geometrical one instead of an approach that requires reparamertizing radius to vary with position than with radius can be beneficial as the later is much harder to visualize without a more formal knowledge of differential equations. It is assumed the particle enters at a radius, r_0, with no initial angle. Then it will oscillate with a frequency:

$$\omega = \frac{qB_z(r=0,z}{m\gamma}) \tag{22}$$

which means that the angular velocity is given in Eq. 13 with $r = r_0$. The radius that the particle will remain at, called the radius of gyration, is:

$$r_\perp = \frac{m\gamma|v_\theta|}{qB_z(r=0,z)} = \frac{r_0}{2} \tag{23}$$

Utilizing the law of sines it is found that:

$$r(z) = r_0 \cos\left(\frac{qB_z(r=0,z-z_0)}{2mv\gamma} \right) \tag{24}$$

$$\frac{\mathrm{d}^2}{\mathrm{d}z^2} r + \left(\frac{B_z\left(r=0,z\right)}{2[B\rho]} \right)^2 r = 0 \tag{25}$$

where again Hill's Equation is reached. Renaming the coefficient to $\kappa(z)$, a matrix analysis can be performed that allows for the transformation of both the radial position, and the rate of change of

radial position with respect to the axial coordinate.

$$\begin{bmatrix} r \\ \frac{\mathrm{d}r}{\mathrm{d}z} \end{bmatrix}_z \approx \begin{bmatrix} 1 & 0 \\ -\frac{1}{f} & 1 \end{bmatrix} \begin{bmatrix} r \\ \frac{\mathrm{d}r}{\mathrm{d}z} \end{bmatrix}_{z_i} \tag{26}$$

The left side of Eq. 26 is the transformed coordinates, at any z, and the right side is the transformation matrix multiplying the original coordinates, at $z = z_0$.

It was mentioned earlier that the solenoid acts as a lens for the electron, much like a pair of glasses bends light into the eye. A property of an optical lens is the focal length. The focal length is the point where light converges, measured from the center of the lens. It can also be thought as a measure of how much the lens bends light; the shorter the focal length, the sharper the lens bends the light. The same characteristics can be applied to the solenoid. The solenoid's focal length is:

$$\frac{1}{f} = \left(\frac{B_z \left(r = 0, z = 0 \right)}{2 \left[B\rho \right]} \right)^2 L = \kappa(0) L \tag{27}$$

From this relationship a very important conclusion can be drawn, and it arises due to the rigidity in the denominator. From Eq. 6, the rigidity is equivalent to the ratio of momentum to charge. That means if the momentum is small or the charge is very large, the lensing effects will be much greater. The latter is a bit harder to visualize, but fact that the lower the momentum the higher the lensing effects is easier to understand. It can be thought of in a system of two soccer balls. Ball 1 is rolling across the field at a given speed, when Ball 2 is kicked into the path of Ball 1 resulting in a collision, and it is assumed that all of the energy of Ball 1 in transferred into Ball 2. If Ball 1's velocity was low compared to Ball 2's, then overall Ball 2's path will not be change that much. If Ball 1's velocity is much higher, then Ball 2's path changes much more. The more the path changes the stronger it is lensed.

The focal length in Eq. 27 will be utilized with Eq. 26 to simulate the path of an electron through the solenoid. The starting coordinates will be input into the right side of Eq. 26, and the coordinates on the left side are the coordinates of the electron after it exits the solenoid. Later,

this matrix will be used in 14 successive iterations, showing the path evolution of the electron It is more useful for calculations if Eq. 26 is resolved into x and y coordinates. Taking directly from Dr. Lund's presentation on this topic [4], and setting $\kappa = k_L^2$, the transform matrix is:

$$\mathbf{M} = \begin{bmatrix} 1 & 0 & 0 & 0 \\ 0 & 1 & -k_L & 0 \\ 0 & 0 & 1 & 0 \\ k_L & 0 & 0 & 1 \end{bmatrix} \begin{bmatrix} 1 & \frac{1}{2k_L}\sin(2k_L L) & 0 & \frac{1}{k_L}\sin^2(k_L L) \\ 0 & \cos(2k_L L) & 1 & \sin(2k_L L) \\ 0 & \frac{1}{k_L}\sin^2(k_L L) & 1 & \frac{1}{2k_L}\sin(2k_L L) \\ 1 & -\sin(2k_L L) & 0 & \cos(2k_L L) \end{bmatrix} \begin{bmatrix} 1 & 0 & 0 & 0 \\ 0 & 1 & k_L & 0 \\ 0 & 0 & 0 & 0 \\ -k_L & 0 & 0 & 1 \end{bmatrix} \tag{28}$$

The previous equation gives the transformation matrix in three parts: the thin lens kicks at the entrance and exit of the solenoid, and the rotation in the central region of the solenoid.

3. RESULTS

3.1 Single Pulse

At each location, 1200 time steps were calculated, collecting a B_x, B_y, B_z, and current value at each time step. This constituted the data collection for one pulse. A single pulse can be seen in Fig. 4. The B_x and B_y values are constant, and constant at a low value, which is what is expected for a solenoid's field.

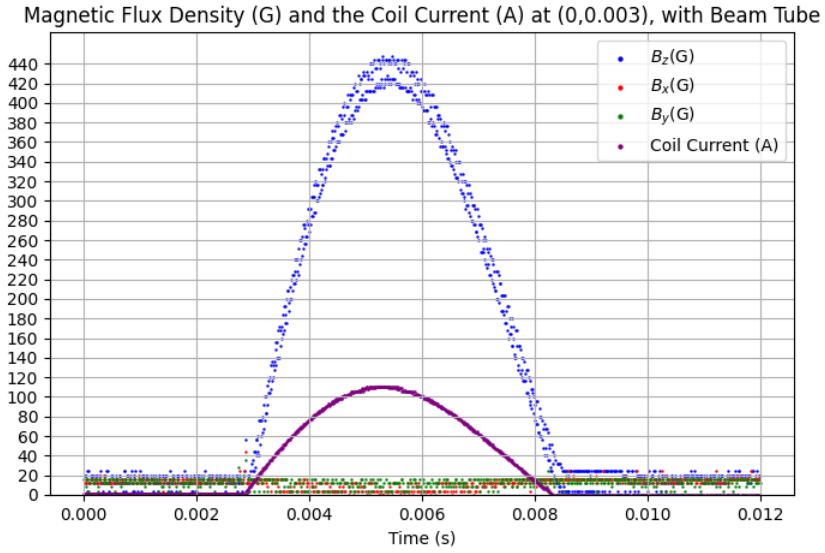

Figure 4: *This is a graphical representation of all of the data points collected during a single current pulse. It is the same data as Fig. 1, but without the black box, as in this case the emphasis is not on the peak, but rather the figure as a whole. The B_x and B_y fields say constant at a very low level as expected, and there is a slight delay between the peak of the B_z and the current.*

3.1.1 Beam Tube vs. No Beam Tube

The effect of the beam tube can best be seen in the plot of the single data point, as in Fig.5. While the currents of each configuration line up very well, the fields are slightly offset. Without the beam tube, the delay between the current peak and the field peak was consistently 40-60 μs,

but once the beam tube is introduced, this jumps to 120-140 μs. This delay was expected, but the exact effects were not predicted. The increased delay is due to the diffusion of the magnetic fields through the material. A good analogy is how a paper towel and a sponge absorb water. Water quickly diffuses through to the other side of the paper towel, but with the sponge requires a much longer time to completely diffuse through to the other side; the same thing is occurring here. When the metal beam tube is in place, the magnetic fields must first diffuse through the beam tube before it can reach its peak values, which is why the delay is seen. The derivation of this magnetic diffusion time constant is not within the purview of this paper and will not be further discussed.

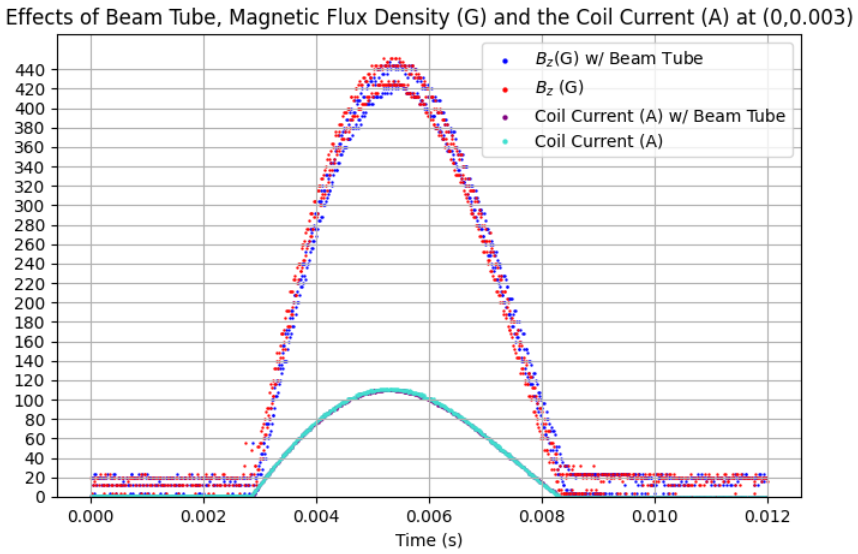

Figure 5: *Comparing the single pulse graphical representations of a single pulse with the beam tube inserted vs no beam tube. The $B_x and B_y$ fields were omitted as they have no impact on the interpretation of the graph and would have only cluttered it. The current peaks occur at the same time regardless of the presence of the beam tube, but the peak in the B_z occurred later when the beam tube was inserted.*

As is only adds a delay to the peak field, and does not change the magnitude of the peak field, the plots of the B_z for the beam tube and no beam tube are identical, which can be seen in Fig. 6. This figure also shows how small B_r is compared to B_z. This can be used to justify the

approximation found in Eq. 5.

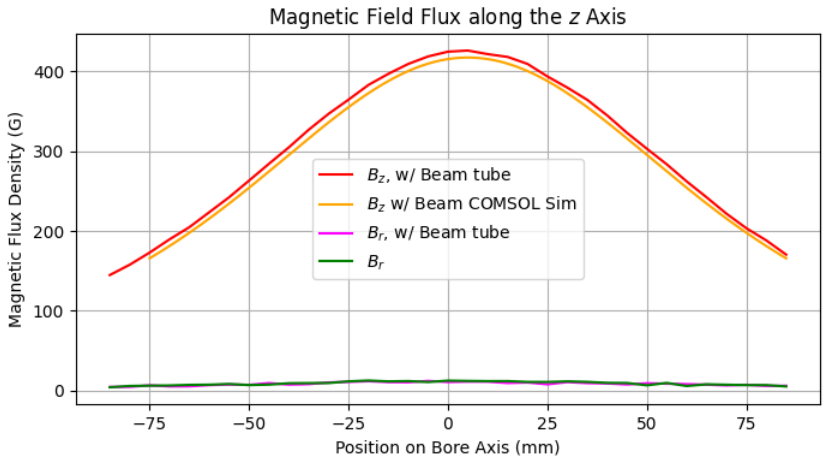

Figure 6: *Comparing the peak measured B values vs the COMSOL simulated values as the position on the z axis change. The B_r (simply a way of writing B_x and B_y together) stays consistent at a low level. In a completely idealized world, B_r would have been 0. The measured values were uniformly offset by a small amount.*

3.2 At r=0, 10mm, and 20mm

In Fig. 7, the effects of the beam tube, or the lack thereof, can be seen. Not only is there no discernible difference between the $+x$ and $-x$, there is no difference between having a beam tube and not having one. Additionally the peak field occurs in the center of the solenoid, which is what should happen inside of a solenoid. This all aligns with the expected results.

3.3 Comparison Between Measured, Simulated, and Predicted Values

The values for the measured, simulated, and predicted fields are all plotted in Fig. 8. In this field there are two significant results. First the predicted value is centered at z=0 mm, whereas the measured and simulated values are slightly offset, centered at z=5 mm. All this means is that when the z=0 point was initially set, it was not set completely flush with the solenoid face as was intended, instead it was set 5 mm into the solenoid. This is further confirmed by manually adding a 5 mm offset in the z direction and replotting the results. This had no effect on the later analysis

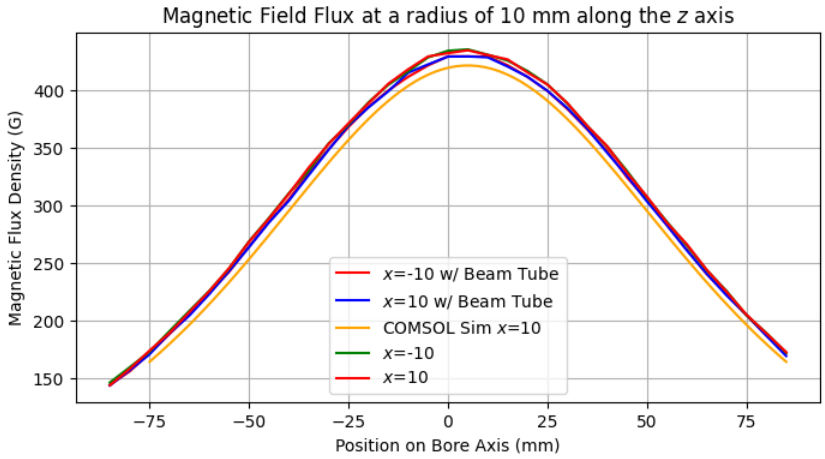

Figure 7: *Comparison of B_z values at $x = \pm 10$ mm, as well as the COMSOL simulation at $x = 10$ mm. They are all the same shape with all of the experiementally measured values offset by the same amount from the simulated values, the same as the result shown in Fig. 6. Because the $x = 10$ and $x = -10$ plots are the same, it can be concluded that the solenoid is symmetric, as desired.*

of the results, it just meant it was slightly offset.

The second significant result shown in Fig. 8 is the slight vertical offset in the measured data and the simulated values, and a much larger offset between those two and the calculated values. The difference between the simulated and the measured values can be much more easily explained. During testing, it was found that the measured values had a uniform and constant offset across all values. During data collection, there were many different current values were tested, so there are more data sets than the one analyzed in this thesis. Different currents were tested not because the improved the gathered data, but the parameters that LLNL wanted changed. As there were different data sets, this mysterious offset was measured an compared with offsets from different data sets. While the offset was not constant across all data sets, it was constant within each set, which was an acceptable finding. As long as it was producing a uniform effect, it meant that nothing was structurally wrong with the setup, and nothing needed to be adjusted.

These results also held true at $r = 10$, which can be seen in Fig. 9. The beam tube made no appreciable difference on the peak field value, which is why the red and blue lines overlap. The offset is also still present at $r = 10$, which is why the yellow line is slightly lower. This is as

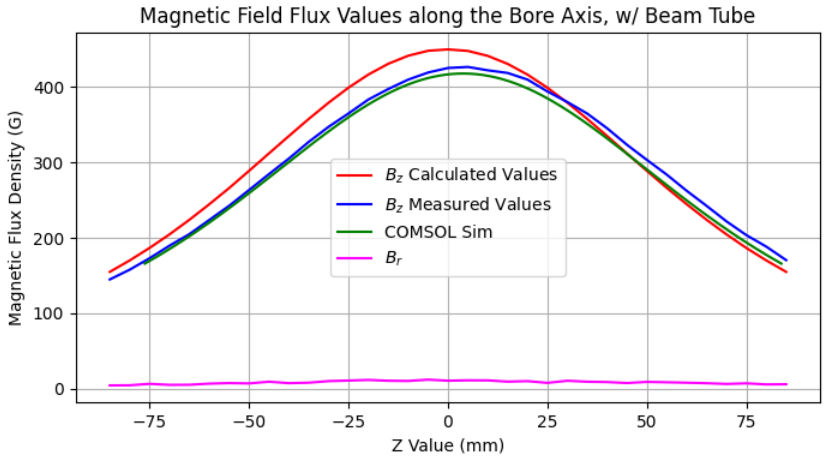

Figure 8: *Comparison between the measured values, calculated values, and the simulated values of B as a function of z, along the bore axis. The calculated values are higher as expected because they were calculated using idealized conditions and simplifications. There is a small horizontal offset between the calculated values and the other two set of values. This is because when the zero point was intially set, it was not perfectly on the face of the solenoid but rather slightly offset. This had no impact on any calculations.*

expected, as what holds true for the bore axis should also hold true on the outer radii.

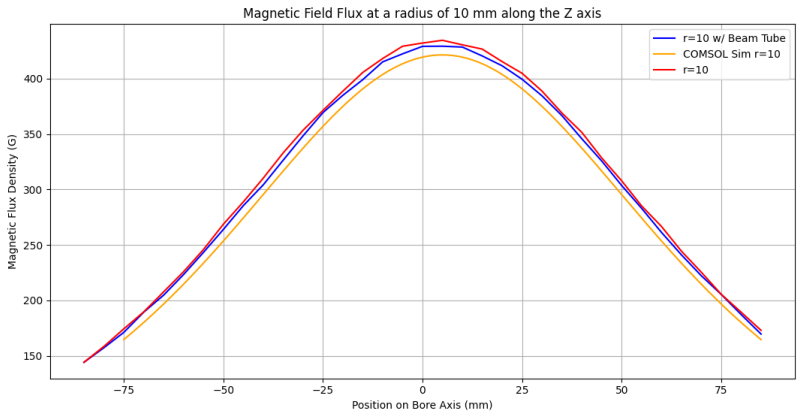

Figure 9: *Comparison between the measured values, calculated values, and the simulated values of B as a function of z, at $r = 10$ mm. The calculated values are higher as expected because they were calculated using idealized conditions and simplifications. There is a small horizontal offset between the calculated values and the other two set of values. This is because when the zero point was intially set, it was not perfectly on the face of the solenoid but rather slightly offset. This had no impact on any calculations.*

3.4 Path Tracing

Using Eq. 28, the motion of the electron through the entire 14 solenoid beam tube is simulated. Through each iteration of the simulation, the exit coordinates of one solenoid is entrance coordinates of the next solenoid. This can be seen in Fig. 10.

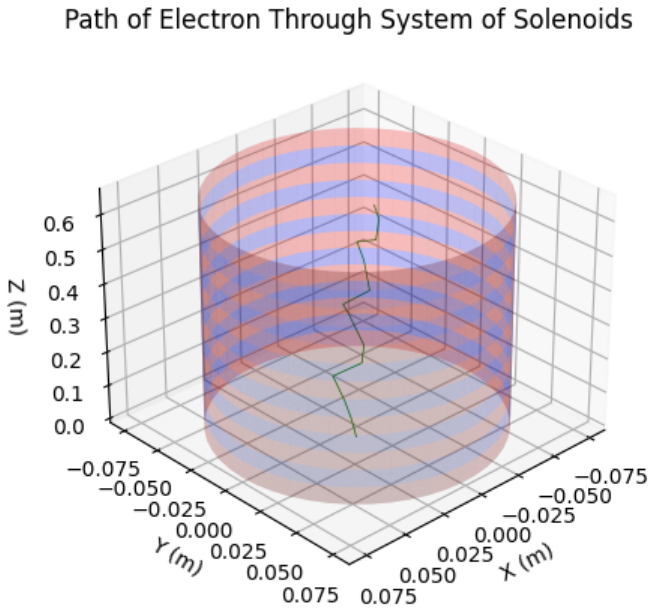

Figure 10: *The path of the electron (green) is shown as it traverses through a path of 14 solenoids. The solenoids are the alternating red and blue cylinders.*

The data in Fig. 10 can be further represented in a two dimensional format in Fig. 11. In this plot, it can be seen that the x coordinates and the y coordinates are oscillating roughly out of phase with each other, seen in the blue and the red respectively. When plotted as a radius, seen in green, it slowly increases as the velocity of the electron increases.

Viewing Fig. 10 along the bore axis results in a view seen in Fig. 12. The particle starts at $(x, y) = (0, 0)$, and they oscillate around the center axis, not quite circular fashion, but in a pattern that appears to precess around the center axis. This result is the one that is expected, as when Fig.

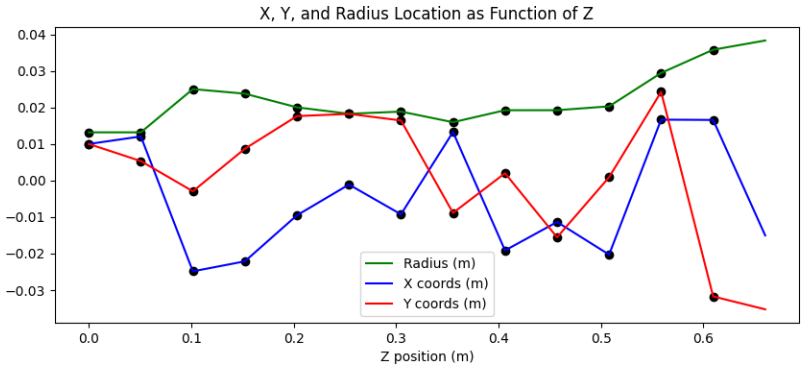

Figure 11: *Two-dimensional readout of the data shown in Fig. 10. The x and y (blue and red) alternate up and down, where the radius as a whole generally trends upwards.*

12 is compared to the result found in the USPAS presentation (seen in Fig. 13), they appear quite similar, albeit a bit rougher as there were not as many points used.

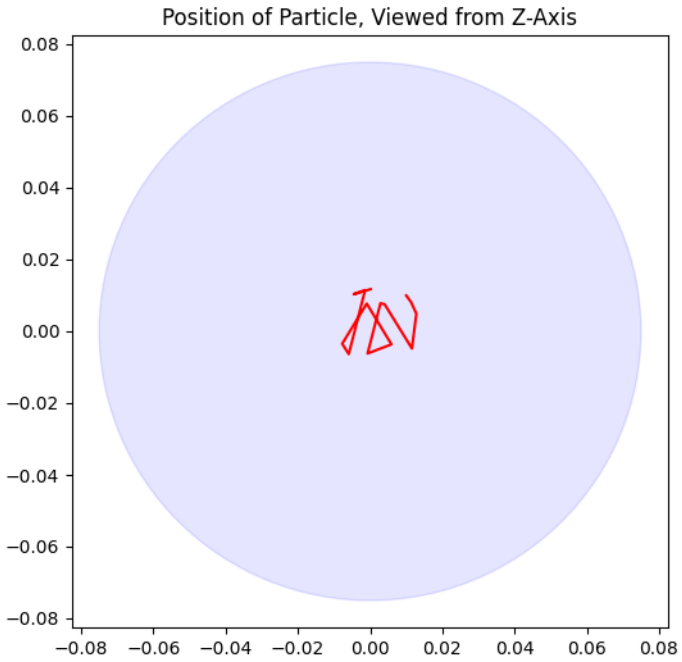

Figure 12: *Top down view of Fig. 10.*

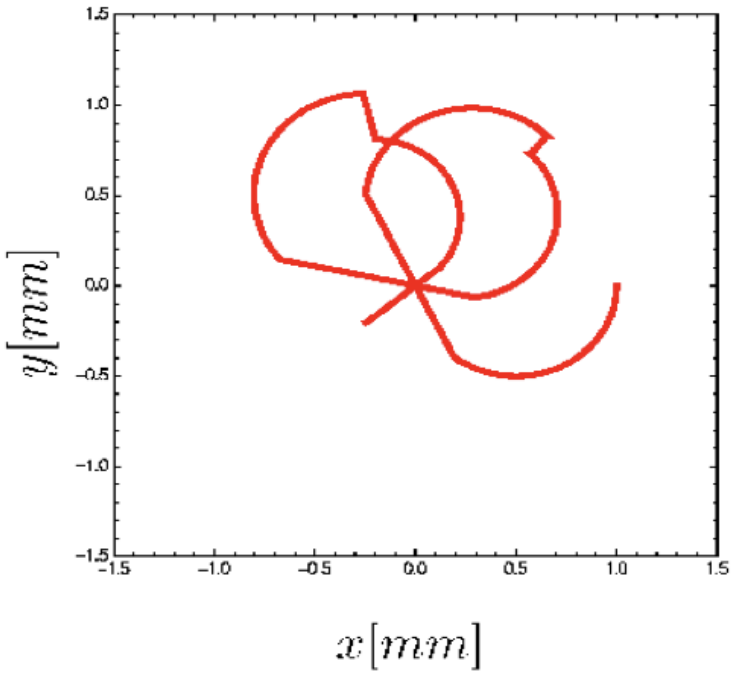

Figure 13: *This is what Fig. 12 should look like under ideal conditions and many data points. This was taken from the USPAS Presentaion on Solenoid Focusing [4]*

By using Eq. 27, the focal length is calculated to be $f = 1.31m$, which satisfies the requirement that $f >> l$, meaning the result can be trusted.

4. CONCLUSION

4.1 Field Mapping Results

The measured field closely aligned with the fields simulated in COMSOL and theoretically predicted. The measured and predicted fields were consistently higher by a few gauss, but this value was consistent for every value in the data set, and was deemed not of concern. By showing that the field values on either side of the solenoid matched, it was also found that there were no asymmetries, as expected. A slight delay in peak field was discovered when comparing results with the beam tube and without, and this arose from the magnetic diffusion through the metal beam tube. Additionally the results were all generated with the magnetic permeability of free space rather than the magnetic permeability of the respective materials. That was just because it greatly simplified the calculations and did not greatly impact the results.

4.2 Particle Path Simulation

The path of the electron was simulated using a simplified and approximated magnetic field, giving results that show the general trend that the exact results would take. The path of the particle was centered along bore axis, and in general the radius increased as it went further down the beam tube. The result was compared to one that was produced in a prior paper, and the results were comparable.

4.3 Further Study

The next steps for this project are to construct a second solenoid, and repeat the same analysis. Those results would then be checked against the results found in this investigation. If they match, the rest of the solenoids would be constructed and verified one final time, and would then be implemented at LLNL. If they are different, a new investigation would be undertaken to find out why these differences are occurring. If the difference was not due a simple error, and it was related to a fundamental flaw, this problem would need to be fixed before any part of the project can be moved forward.

REFERENCES

[1] E. Callaghan and S. Maslen, "The magnetic field of a finite solenoid," *NASA Technical Note D-465*, 1980.

[2] C. Orozco, L. Elementi, S. Feher, H. Friedsam, J. Grudzinski, J. Hejdukova, M. Lamm, J. Nogiec, B. Pollack, T. Strauss, R. Talaga, R. Wagner, J. White, and H. Zhao, "Hall probe calibration system design for the mu2e solenoid field mapping system," *FERMILAB-CONF-17-651-TD*, 2017.

[3] B. Pollack, R. Pellico, C. Kampa, H. Glass, and M. Schmitt, "Modeling magnetic fields with helical solutions to laplace's equation.," *Instruments and Methods in Physics Research Section A: Accelerators, Spectrometers, Detectors and Associated Equipment*, 2020.

[4] S. Lund, "Solenoid focusing." Presentation at US Particle Accelerator School, June 2018.

[5] *Hall Probe C for F3A Magnetic Field Transducers*.

[6] D. J. Griffiths, *Introduction to electrodynamics; 4th ed.* Boston, MA: Pearson, 2013. Republished by Cambridge University Press in 2017.

[7] A. Savitzky and M. J. E. Golay, "Smoothing + differentiation of data by simplified least-squares procedures," *Analytical Chemistry*, 1964.

[8] S. Barletta and Harms, "Transverse dynamics." Presentation at US Particle Accelerator School.